

Fluid Dynamics in Space Sciences

H. Pérez-de-Tejada
Institute of Geophysics, UNAM
Mexico

1. Introduction

Much of what it is understood in nature and that it is also inherent to our common activities can be appropriately interpreted as representing evidence of a collective response that substantiates the basis of fluid dynamics. Such is the case for the behavior for a group of particles or individuals that interact with each other as they follow common trajectories. Under most circumstances their interaction takes place across distances (mean free path) that are much smaller than the size of the region where they move and, as a whole, they exhibit properties (density, speed, temperature) that represent average local values of the conglomerate. Besides the application of this view to standard problems in physics and engineering it has been intuitively suggested that it could also be relevant to describe the motion of the solar wind which at large distances from the sun travels with its particles barely executing any collisions among them. Even though the solar wind is, in fact, a (collisionless) ionized gas it maintains a collective response as it expands through interplanetary space and interacts with the planets of the solar system. The text below describes the manner in which the fluid dynamic interpretation of the solar wind was initiated and how it has expanded to examine its interaction with the planets of the solar system.

2. The solar wind as a continuous expanding gas

The over one million degree temperature of the solar corona is significantly larger than the nearly six thousand degrees of the solar surface and thus provides the energy source that ultimately leads to its strong outward expansion. In fact, the large amounts of energy that are delivered to the solar corona from the solar interior can be mechanically used for producing the solar wind. The prediction and theoretical description of this phenomenon was provided by E. N. Parker ¹ at the University of Chicago who over 50 years ago devised a fluid dynamic interpretation of the manner in which the ionized coronal gas (plasma) is forced to expand outward reaching speeds of the order of 300-400 km/s. A remarkable aspect of this concept is that the solar wind is predicted to be an outflowing continuum gas that expands away from the sun as its density decreases to values that by the earth's orbit are very small ($\sim 10 \text{ cm}^{-3}$). As a result, collisions among its particles (mostly protons and electrons) become extremely rare and the solar wind rapidly becomes a collisionless plasma with an effective mean free path for the collisions of its particles that is comparable to one astronomical unit (this is the distance between the earth and the sun). Despite this constraint observations made with various spacecraft in the interplanetary medium have confirmed the existence of the solar wind and its overall collective response when it interacts with the

planets of the solar system. Much research has been conducted to investigate the processes that allow the solar wind to explain its collective behavior as it moves through space, interacts with the magnetic fields and the ionospheres of planets, and reaches its outer boundary (the heliopause) located at nearly 80 astronomical units.

A fundamental property of the solar wind is that it is rapidly accelerated to reach supersonic speeds and that the process that produces it was incorporated by applying conditions similar to those employed in the fluid dynamic de-Laval nozzle theory. The latter problem serves in rocket engine turbines and is designed to produce supersonic speeds in a streaming flow that is subject to a pressure gradient along its direction of motion. When a subsonic flow is compressed by decreasing the cross-sectional area of the region where it moves its speed increases but remains subsonic. In order to make the flow supersonic it is necessary to introduce a nozzle (converging/diverging) geometry so that the gas first becomes compressed and later expands upon streaming through a "throat" or region of minimum cross-sectional area as it is depicted in Figure 1. The reason here is that when a flow moves into the region of smaller cross-sectional area the imposed pressure gradient can increase the flow speed only up to the sound speed, but a further increase requires an

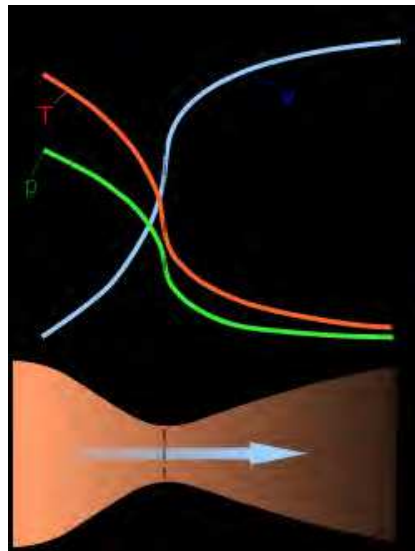


Fig. 1. Scheme of flow through a de-Laval nozzle. The speed profile (blue curve) shows how the flow reaches the sound speed at the throat and becomes supersonic afterwards. The temperature and pressure profiles (labeled T and P) indicate how the gas cools off and expands when it becomes supersonic².

expansion, that is, that the flow proceeds in a diverging geometry. These considerations are better illustrated by the de-Laval equation in hydrodynamics²:

$$ds/s = (v^2/c^2 - 1) dv/v \quad (1)$$

where v is the speed of the flow, s is the cross-section of a duct or region where the flow moves and c is the speed of sound (dv and ds are changes of those variables along the direction of motion). This equation is derived from the continuity and the momentum

equations of the flow and states the correlation that there exists between a change in the speed of the flow and that of its cross-sectional area. Most notable is that when the duct is converging (negative $ds < 0$ values) and the speed of the flow increases (positive $dv > 0$ values) then v must be less than c so that the value of the parenthesis is negative. Such conditions correspond to subsonic flows where the Mach number $M = v/c$ is smaller than one. When $v = c$, that is if $M = 1$, we now have $ds = 0$ and the duct should stop converging. Finally, if v is to exceed c (supersonic flows) then ds must increase ($ds > 0$) for positive changes in the value of the flow speed ($dv > 0$), thus implying that the duct should now be diverging. Such flow conditions of the de-Laval nozzle require, in addition, a large pressure difference along the direction of motion. If that difference is not large, implying that the speed of the flow is slow and does not reach the sound speed at the narrowest part of the duct, then it will only speed up the flow as a Venturi tube achieving only subsonic speeds. The coordinated dependence between changes in the speed of the flow and those in the cross-section of the duct that was derived from equation 1 for the converging/diverging geometry of Figure 1 is a remarkable property that characterizes subsonic and supersonic flows. Its origin lies on the simultaneous consideration of pressure forces that balance the momentum convective term in the momentum equation of the flow from which Equation 1 was derived. On the other hand, even though the presence of the gravitational force and the outward radial expansion of the solar wind in the solar corona leads to flow conditions that are entirely different from those of the two-dimensional flow that streams in the duct of Figure 1, it is significant that a relationship similar to that in Equation 1 can also be derived by employing the continuity and the momentum equations that apply to the solar wind. Following Parker it is possible to replace equation 1 by ³:

$$[2 - MG/(r c^2)] dr/r = (v^2/c^2 - 1) dv/v \quad (2)$$

where M is the solar mass and G the gravitational constant in this relation which holds along the distance r away from the sun. This equation was derived by considering that the gravitational force constricts or chokes the solar wind in a manner similar to the converging section of the de-Laval nozzle in Equation 1; that is, the gravitational force replaces the geometric throat that is not present in the region where the solar wind expands. All in all it is very significant that in the derivation of Equation 2 the gravitational force plays a role similar to that of the geometric throat in Equation 1. The similitude between equations 1 and 2 serves to substantiate the fluid dynamic interpretation of the motion of the solar wind. For example, if the expansion velocity of the solar wind increases outward ($dv > 0$) then for subsonic speeds ($v < c$) we need $MG/(c^2r) > 2$ so that both sides of the equation become negative, and for supersonic speeds ($v > c$) we need $MG/(c^2r) < 2$ in order to make them positive. These conditions imply that there will be subsonic speeds at small r values and supersonic speeds at large r values. The speed of the solar wind will reach the speed of sound at the critical distance $r_c = MG/2c^2$ implying that the solar wind will gradually become supersonic as it moves away from the sun. Measurements conducted with various spacecraft have confirmed this result and, in fact, its observed speed is supersonic being about eight times the speed of sound. It should be noted here that the solar wind will become supersonic at a distance between three and four solar radii, or about two million kilometers above the sun surface. In addition, since the critical distance decreases with increasing the temperature T of the coronal gas, that is by increasing the speed of sound $c = \sqrt{\gamma KT/m}$ where γ is the specific heats of the gas, K the Boltzmann constant and m the mass of the gas particles, then it may occur that the critical distance becomes located below one solar radius if the gas temperature is very high (larger than four million degrees). In that case the solar wind will not reach the sound speed but will

remain subsonic as it expands. Under standard conditions the solar wind becomes supersonic and flows as a continuum gas whose motion is also related to the magnetic field fluxes that are brought up from the sun. As it will be shown below the effects of motion of the solar wind particles in the presence of a magnetic field can be better described by considering the interaction of the solar wind with the earth's magnetic field.

3. The gas dynamic analogue of the solar wind around the earth's magnetosphere

An important contribution to the continuum flow interpretation of the solar wind became available from studies directed to describe its interaction with the earth's magnetic field. That field is, in fact, the effective obstacle that the solar wind encounters as it approaches the earth since its ionized populations (protons and electrons) can be directly influenced by the planetary magnetization. The effect of their interaction is that as a whole the solar wind compresses and deforms the distribution of the earth's magnetic field which becomes bounded in the dayside and is deviated in the nightside forming a magnetic tail that extends far downstream from the earth as it is illustrated in Figure 2. As a result the earth's magnetic

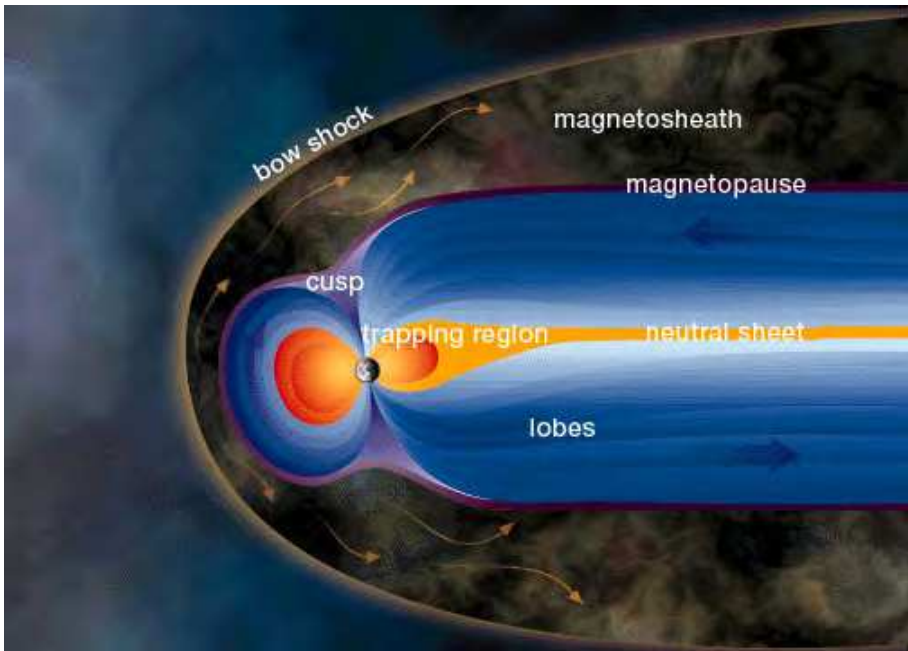


Fig. 2. A schematic view of the earth's magnetosphere formed by the supersonic solar wind that compresses the magnetic field and streams around it as an obstacle after crossing a bow shock front^{3,4}.

field becomes present only within a large confined region in the form of a cavity (called the magnetosphere) whose outer boundary may reach seven earth radii in the direction of the sun. That boundary (the magnetopause) results from a local pressure balance between the solar wind pressure and the compressed pressure of the earth's magnetic field, and implies a

collective response despite the fact that there are no particle collisions in the solar wind population. The mechanism that replaces collisions to allow the transport of information upon encountering the earth's magnetic field is the gyration that the protons and electrons of the solar wind execute when they enter the region occupied by the magnetic field. The process is related to the magnetic (Lorentz) force produced by the magnetic field and the velocity of the particles, and that drives them in a circular (Larmor) motion in a plane transverse to the magnetic field direction. Implied by this motion there is an electric current along the boundary of the magnetosphere that is generated by the different trajectory of the protons and the electrons of the solar wind as they interact with the earth's magnetic field. Their accelerated motion around the magnetic field lines is important because it produces an induced magnetic field whose presence influences the motion of other particles. Thus, despite the fact the solar wind particles are not interacting through collisions with each other there is an ample communication among them which is produced by their motion around the earth's magnetic field lines and that, in the end, justifies its collective response to the presence of that field.

This general idea to view the encounter of the solar wind with earth's magnetic field led J. Spreiter ⁴ and M. Dryer ⁵ to apply a fluid dynamic model available from studies of the interaction of a streaming object in the earth's atmosphere. The purpose of their studies was to describe the manner in which the solar wind encounters the earth's magnetic field and then streams around the magnetospheric cavity. The gas dynamic description of the fluid properties of the solar wind as it reaches the earth's magnetic field and then streams around the magnetosphere is dominated by various features. Most important is a bow shock produced by the supersonic speed of the solar wind and that is located upstream from the magnetosphere in agreement with the common response of a supersonic flow that encounters an obstacle. As it occurs in standard fluid dynamic problems the solar wind decelerates across the bow shock where it also becomes compressed and thermalized reaching values for these properties that are in agreement with those expected from the Rankine-Hugoniot equations of fluid dynamics. As the solar wind streams behind the bow shock and moves around the magnetosphere it gradually recovers its freestream conditions by expanding, cooling and increasing its flow speed as it has been observed with various spacecraft that have probed those regions. As a whole the changes that the solar wind experiences as it interacts with the earth's magnetic field fit adequately with those expected in fluid dynamics.

An evolution of the solar wind similar to that observed around the earth's magnetosphere also occurs when it encounters the magnetic field of other planets. Such is the case for Jupiter, Saturn Uranus and Neptune where their strong intrinsic magnetization leads to large scale magnetospheric cavities and that may reach up to 100 Jovian radii along the sun direction upfront from Jupiter. While comparable large values are also measured for the other planets conditions at Mercury are different where its magnetospheric cavity is very small and only reaches a few thousand kilometers above the surface in the direction of the sun. The solar wind that streams around the magnetic cavity of all these planets bears a similar response in the interaction process.

4. The fluid dynamic interaction of the solar wind with the upper ionosphere of Venus and Mars

4.1 Transport of solar wind momentum to the Venus ionosphere

Unlike magnetized planets Venus and Mars present obstacles to the solar wind that lead to phenomena that are not related to its interaction with a planetary magnetic field. In particular, in the absence of an appreciable intrinsic planetary magnetization the solar wind

does not stream around a magnetic cavity but reaches the upper atmosphere of the planets. The flow conditions are more adequately described as an interaction between two separate bodies of plasma namely, the solar wind and the upper ionosphere. Consequently, the dynamics of the particles that are involved in their interaction is entirely different from that occurring at the boundary of a planetary magnetosphere, and to a large extent it is far more complicated. For example, the access that the solar wind acquires when interacting with particles in a planetary upper ionosphere produces phenomena that do not occur when the solar wind interacts with a planetary magnetic field and suggest the existence of turbulent flow conditions. Information obtained from measurements conducted by spacecraft that have probed Venus and Mars indicate that the interaction between both ion populations seems to be more strongly influenced by turbulent fluid processes rather than through a plasma dynamics similar to that occurring at the boundary of the earth's magnetosphere. There is, in fact, evidence obtained from different sources that suggest the existence of phenomena that strongly resemble those occurring in fluid dynamic problems. A collected view of the various features that have been detected in the Venus plasma environment is presented in Figure 3 from observations conducted with the Pioneer Venus spacecraft (PVO) ⁶. They include, in

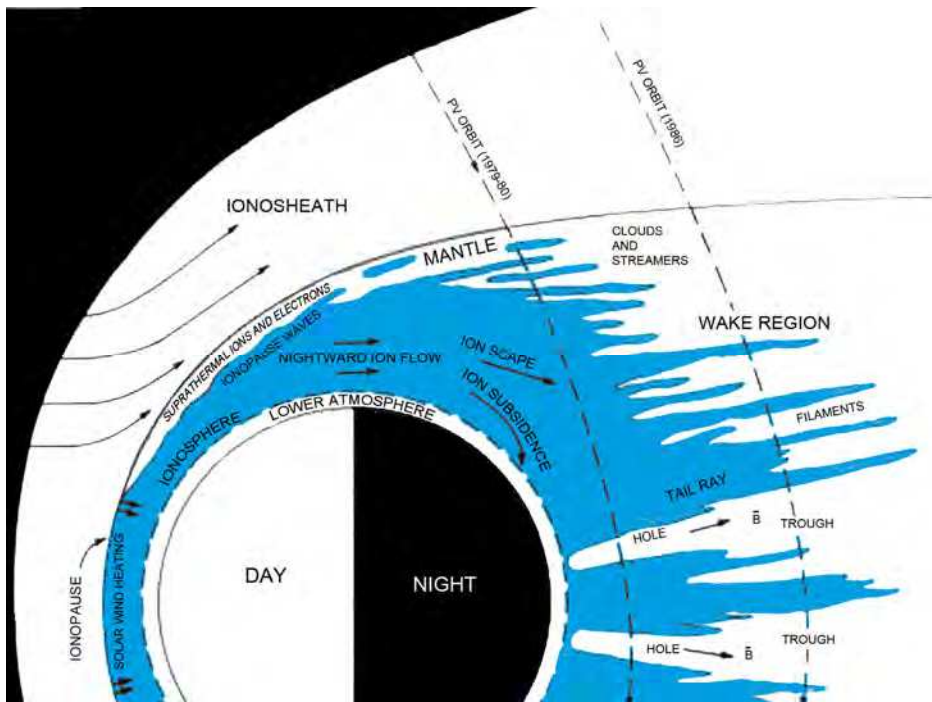


Fig. 3. Schematic diagram of plasma features (bow shock, ionopause, nightward ion flow, tail rays, ionospheric holes) that were identified near Venus with instruments in the Pioneer Venus Orbiter spacecraft (the altitude scale has been enlarged to better describe the geometry of the plasma features)⁶.

addition to a bow shock, plasma clouds or regions of separated ionospheric plasma that imply, in fact, crossings through structures or filaments that extend downstream from Venus. At the

same time there are regions within the nightside ionosphere where there is a large deficiency in the plasma density (ionospheric holes), and equally important is a generalized nightward directed flow of the dayside ionospheric plasma across the terminator.

Studies of the origin of the latter phenomenon (trans-terminator ionospheric flow) have been directed to examine measurements conducted in the region where it has been observed. From the early Mariner 5 spacecraft mission that probed the Venus environment it was learned that the solar wind that flows around the ionosphere exhibits a significant loss of its momentum; that is, its velocity and density show a strong deficit with respect to the freestream values ⁷. That variation is described in the velocity and in the density profiles of the Mariner 5 spacecraft that are shown in the upper panel of Figure 4, and imply that a large fraction of the oncoming energy (shaded regions along the wake) has been removed

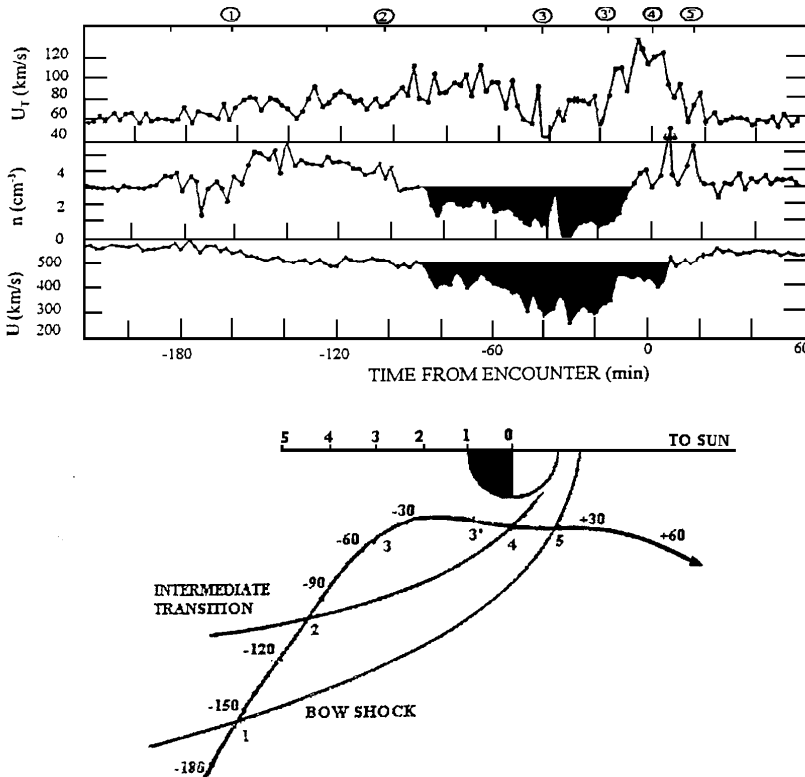


Fig. 4. Thermal speed, density, and bulk speed of the solar wind measured with the Mariner 5 spacecraft (its trajectory projected in cylindrical coordinates is shown in the lower panel). The labels 1 through 5 along the trajectory and at the top of the upper panel mark important events in the plasma properties (bow shock, intermediate plasma transition) ⁷.

from the solar wind. Related information was obtained later from measurements conducted with the Pioneer Venus Orbiter which revealed the ionospheric flow across the terminator that is indicated in the upper panel of Figure 5 and that reaches 3-4 km/s speeds as it is shown in the speed profile in the lower panel of that figure ^{8,9}. The momentum implied by

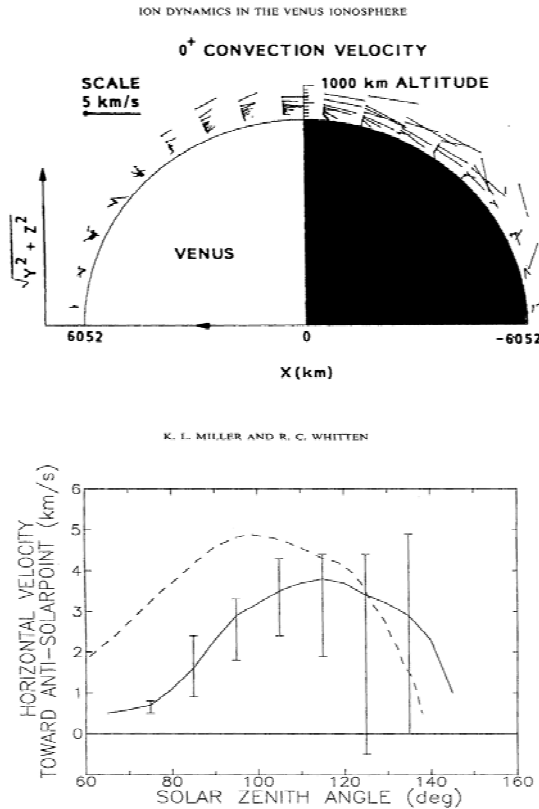


Fig. 5. (upper panel) Average velocity vectors measured in the Venus upper ionosphere with the PVO spacecraft and projected in cylindrical coordinates (the solar wind arrives from the left)⁸. (lower panel). Speed values of the ionospheric particles that move across the terminator at 400 km altitude⁹.

that ionospheric flow is related to the deficit of momentum of the solar wind measured outside the flanks of the ionosphere that is shown in Figure 4. In fact, its kinetic energy density (momentum flux) is comparable to the quantity that was removed from the solar wind; that is, it implies an efficient transport of solar wind momentum to the Venus upper ionosphere¹⁰. Calculations of a momentum conservation equation applied to this problem led to such result which is unrelated to pressure gradient forces across the terminator that have also been suggested to account for the Venus ionospheric flow⁹. The (supersonic) speed of the ionospheric flow and its asymmetry in latitude which is indicated by differences in the extent of the region where the ionospheric plasma is displaced downstream from Venus argues more favorably in terms of momentum transport which mostly occurs by the magnetic polar regions of the Venus ionosphere¹¹. It should be noted in this regard that the "magnetic polar regions" are related to the position where the solar magnetic field fluxes that are convected by the solar wind, and that first pile up around the dayside ionosphere to form a magnetic barrier¹², slip over the planet to take the shape of a hairpin at those regions and then enter the wake¹³. Thus, the outcome of the transport of solar

wind momentum to the Venus upper ionosphere stresses the value of a fluid dynamic view to interpret the interaction between both bodies of plasma despite the fact that it is still necessary to define the mechanisms that through turbulent flow conditions support that behavior.

4.2 Plasma transitions outside the Venus ionosphere

Together with the transport of momentum into the Venus ionosphere the presence of boundaries in the plasma data shown in Figure 4 is indicative of fluid dynamic processes that are operative throughout the region of interaction with the solar wind. As the Mariner 5 spacecraft moved near Venus in its flyby transit from the wake to the dayside (its trajectory projected in cylindrical coordinates is shown in the lower panel of Figure 4) there is clear evidence of two crossings of a bow shock at events labeled 1 and 5. Across the bow shock the speed of the solar wind is smaller in the downstream side (bottom profile in the upper panel), and there is also evidence of heating (larger values in the thermal speed profile labeled U_T) and higher density values (all these variations are similar to those encountered across the bow shock present upstream from the earth's magnetosphere in Figure 2). Equally informative is the observation of a different plasma transition at events labeled 2 and 4 which indicate changes that are not related to a bow shock crossing. In particular, while the solar wind speed further decreases in the downstream side of that transition the density does not increase but exhibits lower values (after event labeled 2 and before event labeled 4). Thus, rather than a bow shock crossing where the solar wind becomes compressed the changes at that plasma transition indicate the presence of a region where the plasma becomes expanded. That transition is not the upper boundary of the ionosphere (the ionopause) which was not crossed by the Mariner 5 spacecraft but a boundary that is innovative since it has not been detected downstream from the bow shock of planetary magnetospheres.

Arguments leading to the presence of the latter transition do not follow from standard views of the acceleration of planetary ions that are generated through the ionization of neutral particles of the Venus atmosphere and that are immersed in the solar wind. In those views the neutral particles that form the planet's exosphere become ionized by the ultraviolet and the x-ray solar radiation and as a result should be rapidly accelerated by an electric field that arises from the relative speed between them and the solar wind¹⁴. The process, named mass loading, is expected to account for the population of planetary ions that is carried by the solar wind and whose contribution should gradually increase with the larger density of exospheric neutral particles that the solar wind encounters when it approaches the Venus atmosphere. While there is clear evidence for the existence of such process there is no indication that it should produce a sharp plasma transition since the accumulation of incorporated planetary ions to the solar wind through mass loading should proceed in a gradual manner¹⁵. Instead, it is necessary to consider that the transition detected downstream from the bow shock in Figure 4 derives from other phenomena, and since it defines the outer boundary of a region adjacent to the ionopause where lower values of the speed and density of the solar wind are measured, it should be related to transport of momentum to the Venus upper ionosphere. In particular, it has been suggested that such plasma transition represents the upper boundary of a region where solar wind momentum is transferred to the Venus ionosphere through viscous forces as it would occur when a streaming flow moves over an obstacle¹⁰. Its position should, therefore, indicate the width of a viscous boundary layer which increases with the downstream distances from Venus as it occurs in comparable fluid dynamic problems.

Further information on the presence of that plasma transitions in the Venus plasma environment has been obtained from spacecraft that have orbited the planet. This is the

case for the Pioneer Venus and more recently for the Venus Express spacecraft whose data have strongly supported the presence of both the bow shock and the plasma transition located downstream from it¹⁶⁻¹⁸. A useful description of recent data is reproduced in Figure 6 from the Venus Express measurements whose trajectory, projected in cylindrical coordinates, is presented in Figure 7. The top and the second panels in Figure 6 show the

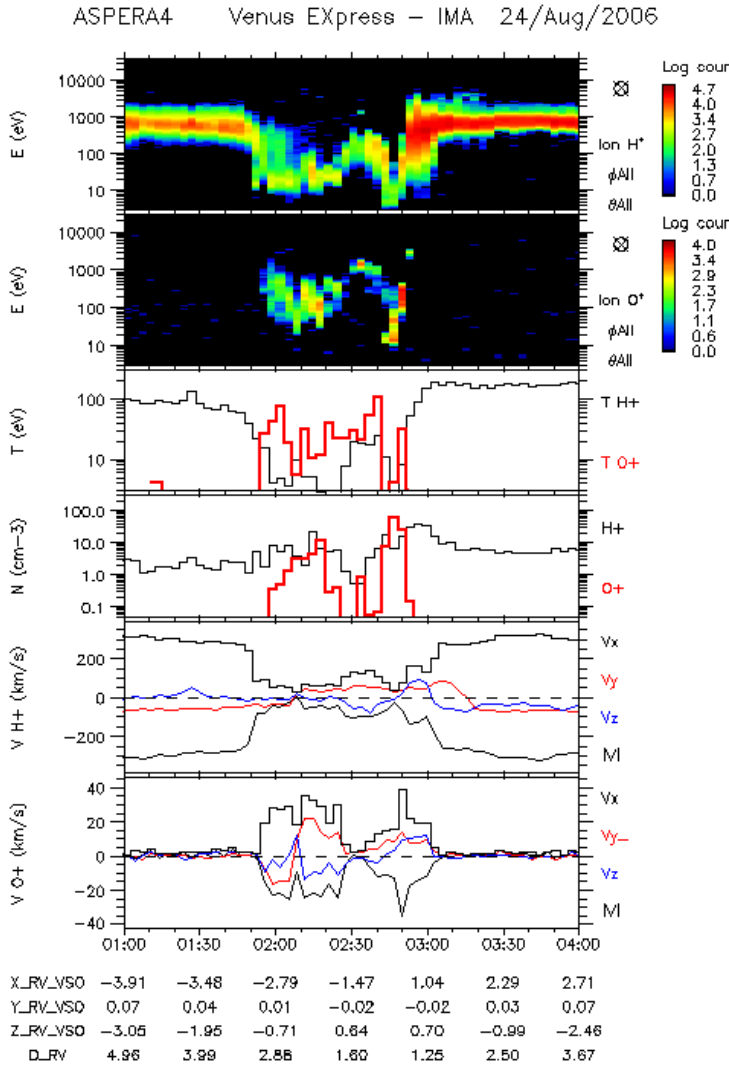


Fig. 6. Energy spectra of H⁺ and O⁺ plasma fluxes (first and second panels) measured in the Venus wake and over the north polar region during orbit 125 of the Venus Express (VEX) spacecraft in August 24, 2006. Temperature and density profiles of both plasma components (third and fourth panels) and their speed V, together with their V_x, V_y, and V_z, velocity components (fifth and sixth panels).

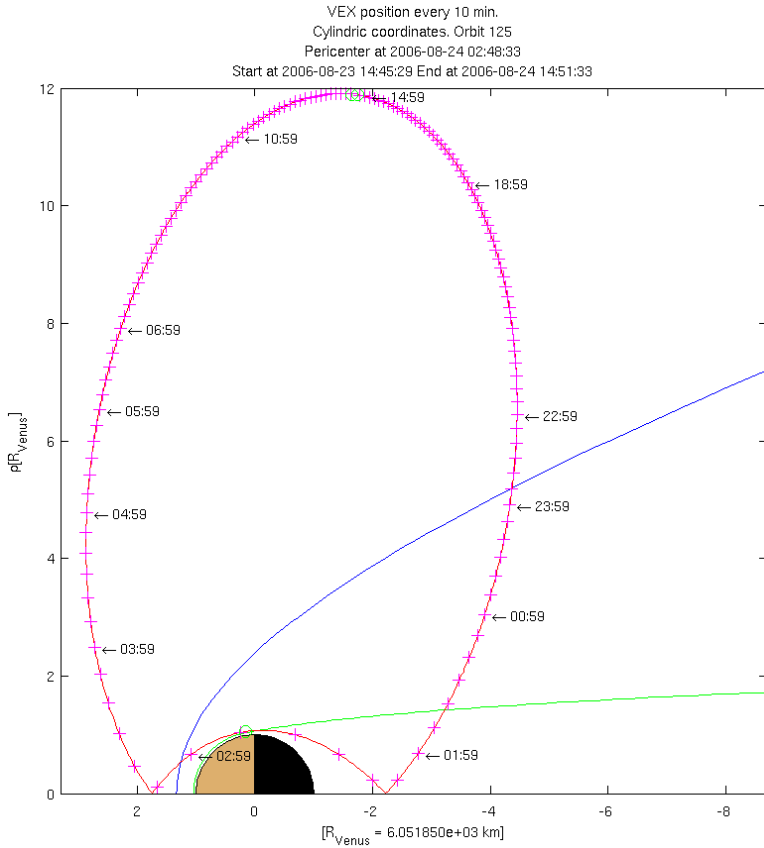


Fig. 7. Trajectory of the Venus Express spacecraft in cylindrical coordinates around Venus during orbit 125 in August 24, 2006,¹⁸.

energy spectra of the solar wind proton (H⁺) population and the planetary ions (mostly atomic oxygen O⁺) that were obtained as the spacecraft moved through the Venus wake in orbit 125 of August 24, 2006. Derived from those spectra are the temperature, density and velocity profiles of both ion components shown in the third, fourth, fifth and sixth panels of Figure 6 from which it is possible to see a bow shock crossing at 03:10 UT (the v_x velocity component in the sun-Venus direction and the speed value of the solar wind H⁺ ions are smaller in the downstream side, and their temperature and density are larger in that side indicating heating and a local compression). Evidence of a separate plasma transition can be identified at 01:52 UT and at 02:52 UT which bound a region where there are even smaller values in the speed of the H⁺ ion population and the observation of O⁺ ion fluxes (red trace). Related to this later plasma transition are the velocity components and the speed value of the planetary O⁺ ions shown in the bottom panel with an important piece of information; namely, their speed (20-30 km/s) is smaller than the local speed (50-150 km/s) of the solar wind H⁺ ions. Different speed values between both ion components would have

not been expected if the planetary O⁺ ions were accelerated by the electric field that, as noted above, arises in the mass loading process (when exospheric neutral particles are ionized their speed is different from that of the solar wind). Rather than reaching solar wind speeds the planetary O⁺ ions maintain small speed values thus suggesting that their motion does not follow gyration around the magnetic field lines as it occurs when they enter a planetary magnetosphere. Instead, their response to local conditions is that they are slowly accelerated through processes that resemble those occurring in turbulent fluid dynamics. The data presented in Figure 6 thus indicates that the interaction of the solar wind with planetary ions in the Venus plasma environment can be viewed in the context of fluid dynamics with processes related to local turbulence and that provide the basis of that approach.

4.3 Plasma channels over the magnetic polar regions of the Venus ionosphere

Observations related to the geometry of the Venus nightside ionosphere and the plasma distribution in the wake are also supportive of a fluid dynamic view since they refer to well defined features that in many instances are present downstream from the planet. Such observations describe plasma clouds and ionospheric holes that were detected as the Pioneer Venus spacecraft moved through the nightside hemisphere within and in the vicinity of the ionosphere. As depicted in Figure 3 plasma clouds are regions that are separated from the main ionosphere and that in fact should be part of ionospheric streamers or filaments that extend downstream from Venus¹⁹. Ionospheric holes are, on the other hand, regions of very low plasma density that in some orbits of the PVO are detected as the spacecraft moves within the nightside ionosphere²⁰. A large fraction of them are measured in the inner wake near the midnight plane but their location is displaced towards the dawn side. A profile of the electron density measured as the PVO moved through the nightside ionosphere in the PVO orbit 530 is shown in the upper panel of Figure 8. That profile describes the ionospheric holes that were detected at 09:30 UT and at 09:40 UT in the northern and in the southern hemisphere along the near polar oriented trajectory of the spacecraft (As it is shown in the lower panel of Figure 8 the lower values of the electron density within the holes are accompanied by enhanced magnetic field intensities)²¹. In some orbits the PVO only detected one ionospheric hole and in others none at all. Their origin and position have been the source of much research and, in particular, they have been interpreted as resulting from plasma channels (or ducts) that the solar wind produces as it moves over the magnetic polar regions of the Venus ionosphere²¹. A schematic view of such plasma channels is illustrated in Figure 9 to describe how they could be sometimes encountered along the PVO trajectory and thus be detected as ionospheric holes. The low density values of the ionospheric plasma within the plasma channels, and hence observed as ionospheric holes, could be due to the erosion that the solar wind produces upon reaching the (magnetic) polar regions. Favorable conditions for a turbulent interaction between the solar wind and the ionospheric plasma in those regions will arise since the local magnetic field intensity is not significantly enhanced as it occurs in the magnetic barrier that builds up around most of the dayside ionosphere¹².

The results of recent analysis of the Venus Express plasma data are also compatible with the presence of plasma channels that extend downstream from the polar regions and thus stress that further research is required to examine its geometric properties such as width, depth, and their evolution along the downstream distance from Venus. Independent of these characteristics it is to be noted that plasma channels in the polar ionosphere provide an important lead on the fluid dynamic interpretation of the data (plasma clouds,

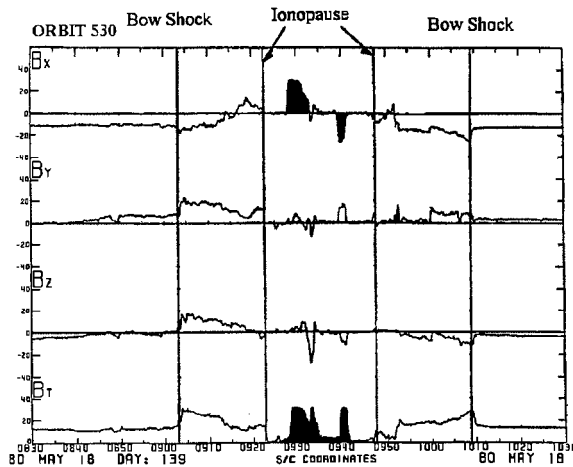
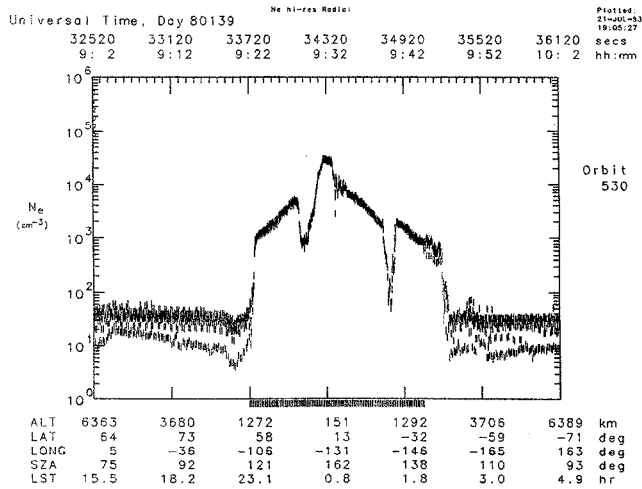


Fig. 8. (upper panel) Electron density profile measured across the nightside ionosphere in orbit 530 of the PVO. The ionospheric holes at 09:30 UT and at 09:40 UT were detected as the spacecraft moved through the northern (inbound pass) and southern (outbound pass) hemispheres²⁰. (lower panel) Magnetic field components and magnetic field intensity B_T measured across the nightside ionosphere in orbit 530 (the shaded areas represent the position of the ionospheric holes)²¹.

ionospheric holes). In particular, while much of the discussion presented here has been directed to describe those features the physical processes that produce them should still be addressed, namely, the manner in which turbulent flow conditions in a collisionless plasma lead to the fluid dynamic behavior.

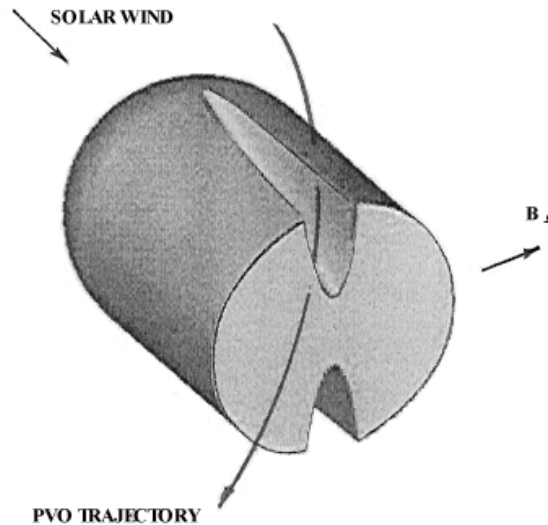


Fig. 9. Schematic view of plasma channels that form by and behind the magnetic polar regions of the Venus Ionosphere ²¹.

4.4 Fluid dynamic Magnus force derived from the rotation motion of the Venus ionosphere

Unrelated to the erosion that the solar wind produces in the upper polar ionosphere there are other observations that also fit within the context of a fluid dynamic interpretation. These refer to a dawn-dusk asymmetry in the distribution of the ionospheric trans-terminator flow as it streams into the nightside hemisphere. Measurements conducted with the PVO show that the flow of ionospheric plasma behind the planet is not seen to converge towards the midnight plane but is oriented to the dawnside of the wake ²². A general description of the manner in which the velocity vectors of the ionospheric flow are traced around and behind the planet (projected on the equatorial plane) is reproduced in the upper panel of Figure 10. As it was noted in Figure 5 the ionospheric flow is mostly measured by and downstream from the terminator but the distribution of the velocity vectors in the upper panel of Figure 10 indicate that the plasma experiences a dawn directed deviation at a $\sim 15^\circ$ angle away from the midnight plane. It is to be noted that the downstream displacement of the trans-terminator flow occurs mostly in the upper ionosphere (between ~ 400 km up to the ~ 1000 km altitude boundary of the ionosphere) and that it is superimposed on a different flow motion that carries the lower ionospheric plasma in the same retrograde rotation of the Venus atmosphere (measurements conducted with the PVO and the Venus Express spacecraft have shown that the neutral Venus atmosphere completes a steady rotation in a 4-5 earth day time span and that this motion is directed in the sense contrary to that of the earth's rotation ²³). Figure 10 shows that the retrograde rotation of the Venus atmosphere is also applicable to the lower ionosphere and hence produces a velocity field that, as it is indicated in the dawn side, is superimposed on the trans-terminator flow. The kinetic energy of the latter flow provides an important contribution to drive the retrograde rotation of the atmosphere ²⁴.

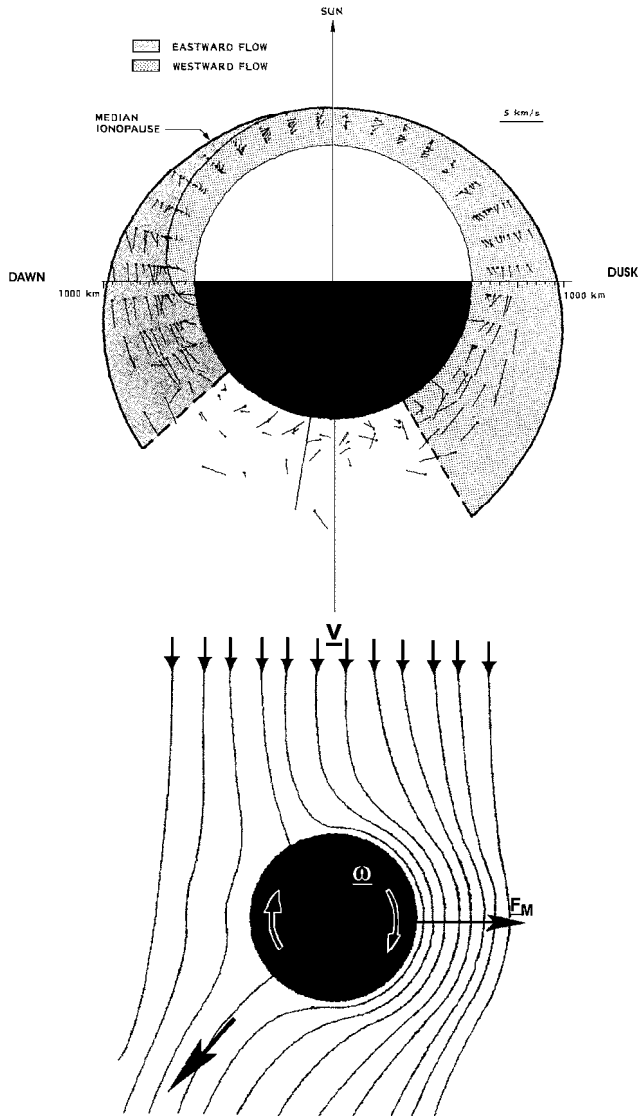


Fig. 10. (upper panel) Velocity averages of the trans-terminator flow and of the rotation of the low altitude ionosphere (which is better seen in the dawn side) that were measured in the Venus ionosphere with the PVO spacecraft and that are projected on the equatorial plane. The velocity vectors of the trans-terminator flow are directed away from the sun (the altitude scale has been increased four times in the figure) ²². (lower panel) Streamline distribution around an obstacle rotating with a frequency ω immersed in a streaming fluid of velocity V . The Magnus Force F_M is directed transverse to the oncoming velocity direction and to the rotation vector ω that points out of the page. The arrow denotes the direction of the deviated wake ²⁶.

The concurrent presence of the rotation motion of an object immersed in a directional flow as that inferred for Venus; namely, the nightward flow of the upper ionosphere and the rotational motion of the lower ionosphere is common in fluid dynamic problems and yields a deflection of the wake that can be used to account for the observations at Venus. A schematic description of the problem is illustrated in the lower panel of Figure 10 which reproduces conditions similar to those presented in the upper panel. The rotation motion of the obstacle produces a velocity field that yields velocity vectors parallel and anti-parallel to those of the directional motion. When they are parallel (right side in the lower panel of Figure 10) the added velocity is large, but becomes small when they are anti-parallel (left side). An important implication derived from the different speed values across the obstacle can be inferred from the Bernoulli's equation:

$$P + \rho v^2 = \text{cst} \quad (3)$$

which implies an inverse relation in the value of the pressure P across the obstacle (ρ is the mass density of the flow) and the kinetic energy of the flow ρv^2 ; that is, low pressure values should be expected in the region where the added flow speed is large (right side in the lower panel of Figure 10) and large pressure values will occur where the added speed is small (left side). In turn, the pressure difference across the obstacle derived from Bernoulli's equation leads to a force (Magnus force) that is responsible for the lateral deviation of rotating baseballs and golf balls in sport activities (curve force) ²⁵. The dawnward directed deflection of the Venus trans-terminator flow indicated in the upper panel of Figure 10 results from the response force that the rotating Venus ionosphere applies on the trans-terminator flow (likewise the deflection of the wake in the lower panel of Figure 10 is produced in response to the Magnus force that the streaming flow applies on the rotating obstacle). Calculations were made to estimate the dawnward directed displacement of the trans-terminator flow produced by the Magnus force when using its 3-4 km/s flow speed and the rotation frequency of the lower ionosphere. The predicted displacement value is of the order of ~ 1000 km for the plasma located in the midnight ionosphere, which compares well with the measurements presented in the upper panel of Figure 10 (the dawnward deflection of the symmetry axis of the trans-terminator flow leads to that value at nightside ionospheric altitudes). In summary, the dawn-dusk asymmetry in the distribution of the trans-terminator flow around Venus is compatible with effects produced by the fluid dynamic Magnus force that applies to a rotating obstacle immersed in a directional flow ²⁶.

4.5 Solar wind erosion of the Mars ionosphere

Much of the interaction of the solar wind with Mars leads to conditions that are similar to those observed at Venus. In the absence of a global intrinsic magnetization in both planets the solar wind reaches their atmosphere and produces phenomena that result in the erosion of their upper ionosphere. This view is applicable around most of Mars but it is modified in the vicinity of regions where there are fossil magnetic fields possibly remnants of an early global field ²⁷ (in those regions the solar wind interacts with small scale magnetospheres of the type generated by the earth's magnetic field). Conditions over the polar regions of the Mars ionosphere resemble those at Venus with ionospheric plasma being removed by the direct access of the solar wind. Information that supports the erosion of the Mars polar ionosphere was obtained from remote observations conducted with the XMM Newton

satellite in orbit around the earth. A long time span image of Mars observed in the x-ray spectrum is presented in Figure 11 to describe the configuration of the region that has been eroded by the solar wind ²⁸. Most notable is the prominent plasma bulge that extends several thousand kilometers downstream from the Mars over the polar regions, and that is

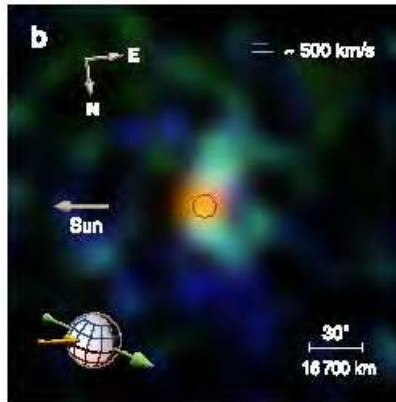


Fig. 11. View of the x-ray emission line halo around Mars measured with the reflecting grating spectrometer (RGS) of the XMM-Newton satellite. The halo is most prominent above the poles and is tilted away from the Sun. The sphere at the lower left indicates the direction of motion of Mars (green arrow) and the velocity of the solar wind particles (yellow arrow) ²⁸.

similar to those occurring at the Venus polar regions. At Mars the solar wind carves out plasma channels with ionospheric plasma being continuously removed within a funnel cross-section that expands away from the wake. A comparable erosion of plasma also occurs by the polar regions of the Venus ionosphere as the channels are maintained open. However, because of the smaller gravitational force of Mars the density of the eroded plasma in that planet should be larger than at Venus, thus yielding evidence of the notable asymmetric plasma halo that is seen in its x-ray spectrum. The x-ray emission in the Mars spectrum corresponds to high energy electron transitions that imply very high temperatures. Calculations made from the emission line distribution in the x-ray Mars spectrum lead to temperature values of the order of one million degrees which may be produced through dissipation processes associated with the transport of solar wind momentum to the polar ionospheric plasma, as it was also suggested for Venus ²⁹. The remarkable shape of the Mars plasma halo shown in Figure 11 represents visible evidence of phenomena that substantiate the value of fluid dynamics in the interpretation of the solar wind interaction with planetary ionospheres. The collective removal of ionospheric plasma from the planets Venus and Mars through erosion processes is a useful byproduct of turbulent flow conditions that allow fluid dynamics to become applicable.

5. Concluding remarks

Much of what has been discussed in regard to the fluid dynamic view of the origin of the solar wind, its expansion through interplanetary space, and its interaction with the planets of the solar system leads to processes that are related to the motion of charged

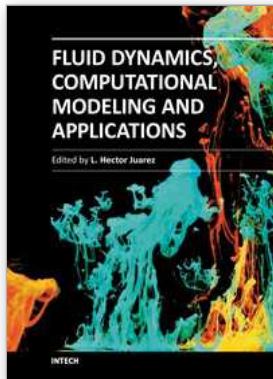
particles through magnetic fields and/or are subject to turbulent flow conditions. In the first case the solar wind particles enter the earth's magnetic field and produce electric currents that bound a cavity in which the magnetic field is compressed and is deformed to produce a magnetic tail. In the latter case the solar wind reaches planetary ionospheres where instead of gyration motion around the magnetic field lines the plasma particles describe stochastic trajectories produced by local turbulence and that suggest the existence of wave-particle interactions. The outcome of this latter activity is the onset of phenomena that can be interpreted in terms of those occurring in fluid dynamic problems. A process that has been applied in this context is the transport of solar wind momentum that occurs along the flanks of planetary ionospheres as it is shown in Figure 4 (the boundary traced between events 2 and 4 represents the outer extent of a viscous layer). For those conditions it has been possible to estimate the viscosity coefficient of the solar wind that is suitable to account for the observations. The calculated values of the kinematic viscosity of the solar wind suggest that they are compatible with the plasma properties of the solar wind; namely, an efficient transport of momentum across a thick ($\sim 10^3$ km) viscous boundary layer measured by the terminator and that is produced under its very low particle densities. In fact, since the value of the kinematic viscosity coefficient ν describes the ability of a flow to modify a velocity profile³⁰ the small density of the solar wind leads to large $\nu \sim 10^4$ km²/s values when compared with those of comparable fluid dynamic problems³¹. Empirical values of the kinematic viscosity of the solar wind are derived on the basis that local turbulence produced by wave-particle interactions provide the origin of the fluid dynamic interpretation^{7, 32}. However, while there are various phenomena that substantiate this view it is still necessary to determine the mechanisms that produce such interactions which lead to the collective response of the solar wind. A required source of information would be obtained from a statistical mechanics applicable to wave-particle interactions and that could provide in mathematical form expressions for the transport coefficients. Much theoretical research should be conducted to improve the information that is now available.

6. References

- [1] Parker, E. N., *Interplanetary Dynamic Processes*, John Wiley, 1963.
- [2] Liepmann, H. W. and A. Roshko, *Elements of Gas dynamics*, John Wiley, 1967 (Chapter 2, p. 52).
- [3] Dessler, A. J., *Solar Wind and Interplanetary Magnetic Field*, *Reviews of Geophysics*. 5,1, 1967.
- [4] Spreiter, J., et al., *Hydromagnetic flow around the magnetopause*, *Planetary Space Sciences*, 14, 223, 1966.
- [5] Dryer, M., et al., *Magnetogasdynamic conditions for a closed magnetopause*, *American Institute Aeronautics Astronautics Journal (AIAA)*., 4, 246, 1966.
- [6] Brace, L., et al., *The Ionotail of Venus: Its configuration and evidence for ion escape*, *Journal of Geophysical Research*, 92, 15, 1987.
- [7] Bridge H., et al., *Plasma and magnetic fields observed near Venus*, *Science*, 158, 1669, 1967.
- [8] Knudsen, W., et al., *Improved Venus ionopause: Comparison with measurements*, *Journal of Geophysical Research*, 87, 2246, 1982.

- [9] Whitten, R. et al., Dynamics of the Venus ionosphere: A 2D model study, *ICARUS*, 60, 317, 1984.
- [10] Pérez-de-Tejada, H., Fluid dynamic constraints of the Venus ionospheric flow, *Journal of Geophysical Research*, 91, 6765, 1986.
- [11] Pérez-de-Tejada, H. Friction layer in the plasma channels of the Venus ionosphere, *Advances of Space Research*, 36, 2030, 2005.
- [12] Zhang, T., J. Luhmann, and C. Russell, The magnetic barrier at Venus, *Journal of Geophysical Research*, 96, 11145, 1991.
- [13] Pérez-de-Tejada, H., et al., Plasma distribution in the Venus near wake, *Journal of Geophysical Research*, 88, 9109, 1983.
- [14] Breus, T. et al., Solar wind mass-loading at comet Halley, *Geophysical Research Letters*, 14, 499, 1987.
- [15] Intriligator, D., Observation of mass addition in the Venusian ionosheath, *Geophysical Research Letters*, 9, 727, 1982.
- [16] Slavin, J., et al., The solar wind interaction with Venus: PVO-Venus bow shock, *Journal of Geophysical Research*, 85, 7625, 1980.
- [17] Pérez-de-Tejada, H., et al., Intermediate transition of the Venus ionosheath, *Journal of Geophysical Research*, 100, 14523, 1995.
- [18] Pérez-de-Tejada, H. et al, Plasma transition at the flanks of the Venus ionosheat: Evidence from the Venus Express, *Journal of Geophysical Research*, 116, A01103, 2011.
- [19] Brace, L, et al., Plasma clouds above the ionosphere of Venus and their implications *Planetary Space Sciences*, 30, 29, 1982.
- [20] Brace, L., et al., Holes in the nightside ionosphere of Venus, *Journal of Geophysical Research*, 87, 199, 1982.
- [21] Pérez-de-Tejada, H., Plasma channels in the Venus nightside ionosphere, *Journal of Geophysical Research*, 109, A04106, 2004.
- [22] Miller, K., and R. Whitten, Ion dynamics in the Venus ionosphere, *Space Science Reviews*, 55, 165, 1991.
- [23] Schubert, G., et al., Structure and circulation of the Venus atmosphere, *Journal of Geophysical Research*, 85, 8007, 1980.
- [24] Lundin, R. et al., Ion flow and momentum transfer in the Venus environment, *ICARUS* (in press, 2011).
- [25] Rouse, H., *Elementary Mechanics of Fluids*, chap. IX, Dover, Mineola, N.Y. 1978.
- [26] Pérez-de-Tejada, H., The Magnus force in the Venus ionosphere, *Journal of Geophysical Research*, 111, A11105, 2006.
- [27] Acuña, M., et al., Global distribution of crustal magnetization at Mars, *Science*, 184, (5357), 790, 1999.
- [28] Dennerl, K., et al., First observation of Mars with XMM-Newton, *Astronomy and Astrophysics*, 451, 709, 2006.
- [29] Pérez-de-Tejada, H. et al, Solar wind erosion of the Mars polar ionosphere, *Journal of Geophysical Research*, 114, A02106, 2009.
- [30] Batchelor, G. K. *An Introduction to Fluid Dynamics*, Cambridge University Press (p. 36), 1979.

- [31] Pérez-de-Tejada, H., Viscous forces in a boundary layer at the Venus ionosphere, *Astrophysical Journal*, 525, L65, 1999.
- [32] Vörös, Z., et al., Intermittent turbulence, noisy fluctuations, and wavy structures in the Venusian magnetosheath and wake, *J. Geophys. Res.-Planets*, 113, E00B21, doi:10.1029/2008, 2008.



Fluid Dynamics, Computational Modeling and Applications

Edited by Dr. L. Hector Juarez

ISBN 978-953-51-0052-2

Hard cover, 660 pages

Publisher InTech

Published online 24, February, 2012

Published in print edition February, 2012

The content of this book covers several up-to-date topics in fluid dynamics, computational modeling and its applications, and it is intended to serve as a general reference for scientists, engineers, and graduate students. The book is comprised of 30 chapters divided into 5 parts, which include: winds, building and risk prevention; multiphase flow, structures and gases; heat transfer, combustion and energy; medical and biomechanical applications; and other important themes. This book also provides a comprehensive overview of computational fluid dynamics and applications, without excluding experimental and theoretical aspects.

How to reference

In order to correctly reference this scholarly work, feel free to copy and paste the following:

H. Pérez-de-Tejada (2012). Fluid Dynamics in Space Sciences, Fluid Dynamics, Computational Modeling and Applications, Dr. L. Hector Juarez (Ed.), ISBN: 978-953-51-0052-2, InTech, Available from: <http://www.intechopen.com/books/fluid-dynamics-computational-modeling-and-applications/fluid-dynamics-in-space-sciences>

INTECH

open science | open minds

InTech Europe

University Campus STeP Ri
Slavka Krautzeka 83/A
51000 Rijeka, Croatia
Phone: +385 (51) 770 447
Fax: +385 (51) 686 166
www.intechopen.com

InTech China

Unit 405, Office Block, Hotel Equatorial Shanghai
No.65, Yan An Road (West), Shanghai, 200040, China
中国上海市延安西路65号上海国际贵都大饭店办公楼405单元
Phone: +86-21-62489820
Fax: +86-21-62489821

© 2012 The Author(s). Licensee IntechOpen. This is an open access article distributed under the terms of the [Creative Commons Attribution 3.0 License](#), which permits unrestricted use, distribution, and reproduction in any medium, provided the original work is properly cited.